

# Non-Fourier Spatial Encoding for Improved Point-Spread-Functions in Hyperpolarized $^{13}\text{C}$ CSI Acquisitions

A. P. Chen<sup>1</sup>, R. E. Hurd<sup>2</sup>, and C. H. Cunningham<sup>3,4</sup>

<sup>1</sup>GE Healthcare, Toronto, ON, Canada, <sup>2</sup>GE Healthcare, Menlo Park, CA, United States, <sup>3</sup>Imaging Research, Sunnybrook Health Sciences Centre, Toronto, ON, Canada, <sup>4</sup>Medical Biophysics, University of Toronto, Toronto, ON, Canada

**INTRODUCTION:** Metabolic imaging using pre-polarized substrates labeled with a  $^{13}\text{C}$  nucleus has proven to be a promising new tool (1). Often, chemical-shift imaging (CSI) acquisitions are used to map the  $^{13}\text{C}$  resonances over 2D or 3D volumes so that  $^{13}\text{C}$  metabolic data from various tissues can be compared. Due to the time constraints imposed by the relatively short lifetime of the hyperpolarized state, the spatial dimensions of these acquisitions are often encoded with small matrix sizes (e.g.  $8 \times 8 \times 16$ ), resulting in a relatively poor point-spread function (PSF). In this abstract, we have explored the use of non-Fourier spatial encoding to improve the PSF in both in-plane dimensions of hyperpolarized  $^{13}\text{C}$  CSI acquisitions.

**THEORY:** Non-Fourier spatial encoding makes use of RF pulses as well as gradients to encode spatial information. One advantage of this is the ability to shape the PSF, improving its localization. In this work, we have combined the PSF-Choice technique introduced by Panych et al. (2) with a Hadamard-like technique to encode the two in-plane dimensions, respectively. PSF-Choice uses a 2D RF pulse that is heavily undersampled in one dimension, resulting in replication of the excitation profile across the FOV in the direction of the undersampling. These replicated excitation profiles form the basis functions for spatial encoding one dimension of the FOV. To encode the other in-plane dimension, the fully sampled dimension of the 2D RF pulses can be used to excite multiband excitation profiles in a manner similar to Hadamard encoding. Instead of Hadamard basis functions, discrete Fourier transform (DFT) basis functions (3) were used in the implementation described below. This had the advantage that the usual Fourier-transform reconstruction could be used with the new method as well as the conventionally acquired data below.

**METHODS:** RF and gradient waveforms for encoding a 5.6 cm FOV with a grid of  $8 \times 8$  voxels were designed in Matlab (The Mathworks Inc.). The 64 different RF pulses and 2 (x and y) gradient waveforms were saved in short integer format. An example RF pulse and the two gradient waveforms are shown in Fig. 1. Bloch equation simulations were performed to compute the PSF resulting from these pulses.

A double spin-echo CSI pulse sequence (4) was modified to load these files and step through the different pulses during the x and y phase-encoding loops. Experiments were performed on a GE MR750 3T whole-body scanner equipped with the broadband package using a custom-built dual-tuned  $^{13}\text{C}/^1\text{H}$  transmit-receive RF coil (Magvale LLC, San Francisco).

To test the quality of the PSF, a phantom experiment was performed using 3 mL syringe filled with 2.7 M [ $1\text{-}^{13}\text{C}$ ] glycine. Data were acquired with non-Fourier encoding as well as conventional phase encoding for comparison.

In vivo data were acquired from a  $\sim 300\text{g}$  Sprague-Dawley rat, with the non-Fourier CSI pulse sequence started 20 s after the start of the injection of 2.0 mL of 80 mM pre-polarized pyruvate through a tail-vein catheter. For this experiment the FOV was 6.4 cm.

**RESULTS:** Simulated excitation profile from one of the 64 pulses designed for the  $8 \times 8$  non-Fourier spatial encoding and reconstructed PSF from this scheme are shown in Fig.2. Excellent PSF is achieved in both spatial dimension with the proposed method. Phantom 2D CSI data (Fig.3) demonstrated improvement in localization of the non-Fourier spatial encoding as compared to standard phase encoding.

**CONCLUSIONS:** A non-Fourier method for spatial encoding (in two spatial dimension) in CSI acquisitions for pre-polarized  $^{13}\text{C}$  metabolic studies was developed and demonstrated. Phantom experiments showed an improved point-spread function and a rat study showed the feasibility of using the method for in vivo data acquisition.

**REFERENCES:** 1. Golman K. et al. PNAS 2006;103:11270-11275. 2. Panych LP. et al. MRM 2005;54:159168. 3. Cunningham CH et al. MRM 2001 45:118-127 4. Cunningham CH. et al. 2007, JMR 2007;287:357-62.

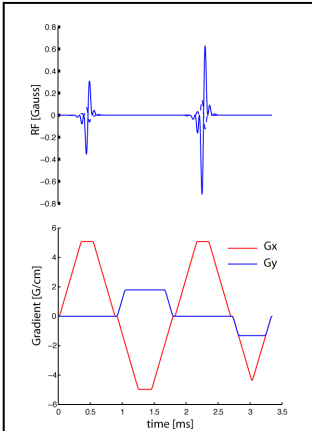


Figure 1. Example RF pulse and gradient waveform (1 of 64). Similar to the original PSF-Choice implementation, the RF excitation consists of two RF pulses whose relative amplitude is varied as the y phase-encode steps are acquired. However, here the individual RF pulses excite multiple bands with relative phases corresponding to the elements of a DFT encoding matrix.

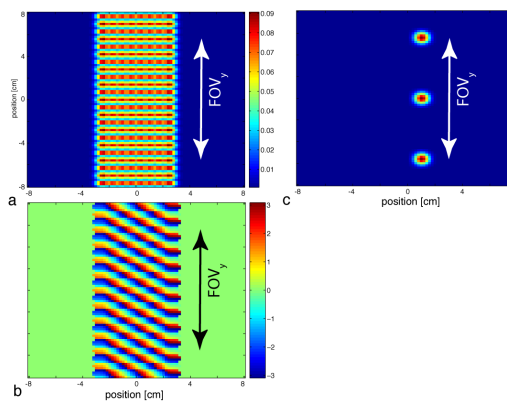


Figure 2. Example excitation profile and reconstructed point-spread function. The (a) magnitude and (b) phase of one out of the 64 excitation profiles is shown. The maximum transverse magnetization in (a) is approximately 0.1 corresponding to the desired tip angle of 10 degrees. The phase profile is scaled in radians. (c) The reconstructed PSF shows excellent localization in both dimensions, with the expected aliasing at the edge of the FOV seen as the replicated PSF at the top and bottom.

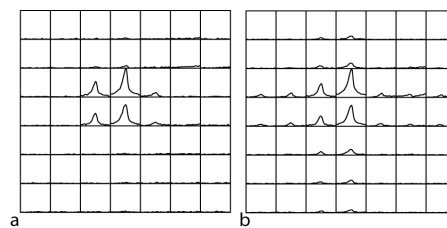


Figure 3. Phantom experiment showing the improvement in the PSF resulting from non-Fourier spatial encoding. The grid shows the spatial distribution of the glycine peak, with the non-Fourier acquisition (a) showing notably better localization compared with conventional phase encoding (b).

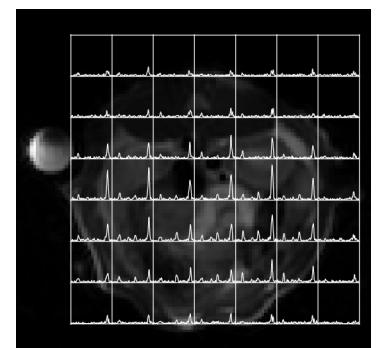


Figure 4. In vivo experiment showing the performance of the non-Fourier method. The spatial distribution of signals after the injection of pre-polarized pyruvate in a slice through the kidneys of a rat is shown.